

## Non-metallic transport in molecular solids versus dimensionality

This article has been downloaded from IOPscience. Please scroll down to see the full text article.

2001 J. Phys.: Condens. Matter 13 2437

(<http://iopscience.iop.org/0953-8984/13/11/302>)

View [the table of contents for this issue](#), or go to the [journal homepage](#) for more

Download details:

IP Address: 171.66.16.226

The article was downloaded on 16/05/2010 at 11:39

Please note that [terms and conditions apply](#).

# Non-metallic transport in molecular solids versus dimensionality

**Marco Zoli**

Istituto Nazionale di Fisica della Materia, Dipartimento di Matematica e Fisica,  
Università di Camerino, 62032 Camerino, Italy

E-mail: zoli@campus.unicam.it

Received 27 November 2000, in final form 1 February 2001

## Abstract

Path integral techniques and the Green's function formalism are applied to study the time- and temperature-dependent scattering of a polaronic quasiparticle using a local anharmonic potential in a bath of diatomic molecules. The electrical resistivity has been computed for any molecular lattice dimensionality for different values of the electron–phonon coupling and intermolecular forces. A broad resistivity peak with non-metallic behaviour at temperatures larger than  $\simeq 100$  K is predicted by the model for sufficiently strong polaron–local potential coupling strengths. This peculiar behaviour, ascribed to purely structural effects, is favoured for low dimensionality.

## 1. Introduction

A considerable amount of theoretical work has been devoted to investigating the conditions required for polaron formation [1–6] and the polaronic features of real materials [7–10]. While there is growing evidence that fundamental properties such as the polaron size, effective mass and ground-state energy are essentially similar in any dimension [11, 12], it is still unclear to what extent transport properties of polaronic systems (in particular, the electrical resistivity behaviour versus temperature) depend on the lattice structure and dimensionality. Besides being conceptually relevant, this question has become of practical interest in connection with the discovery of unusual effects in underdoped high- $T_c$  superconductors. In fact, the presence of local lattice distortions causing polaron formation in high- $T_c$  systems has been envisaged and signs of enhanced anharmonicity for some in-plane and out-of-plane oxygen modes have been detected in underdoped compounds by several groups [13, 14]. In this paper we focus on the problem of the interaction between a polaronic quasiparticle moving through a molecular lattice and a local structural instability modelled by a double-well potential in its two-state configuration. In particular, we derive the effective interaction strengths arising from this peculiar scattering mechanism and we study the effects on the electrical resistivity both of the intermolecular forces and of the lattice dimensionality.

## 2. The model

Our analysis starts from the following  $\tau$ -dependent Hamiltonian, where  $\tau$  is the time which scales as an inverse temperature according to the Matsubara Green's function formalism:

$$\begin{aligned}
 H_0(\tau) &= \bar{\epsilon}(g)\tilde{c}^\dagger(\tau)\tilde{c}(\tau) + \sum_q \omega_q a_q^\dagger(\tau)a_q(\tau) + H_{TLS}(\tau) \\
 (H_{TLS}(\tau)) &= \begin{pmatrix} 0 & \lambda Q(\tau) \\ \lambda Q(\tau) & 0 \end{pmatrix} \\
 H_{int}(\tau) &= -2\lambda Q(\tau)\tilde{c}^\dagger(\tau)\tilde{c}(\tau) \\
 Q(\tau) &= -Q_0 + \frac{2Q_0}{\tau_0}(\tau - t_i).
 \end{aligned} \tag{1}$$

$H_0(\tau)$  is the free Hamiltonian encompassing the following:

- a polaron created (destroyed) by  $\tilde{c}^\dagger(\tau)$  ( $\tilde{c}(\tau)$ ) in an energy band  $\bar{\epsilon}(g)$  whose width decreases exponentially on increasing the strength of the overall electron-phonon coupling constant  $g$ ,  $\bar{\epsilon}(g) = D \exp(-g^2)$ ;
- a lattice of diatomic molecules whose phonon frequencies  $\omega_q$  are derived analytically for a linear chain, a square lattice and a simple cubic lattice through a force-constant model;
- a local anharmonic potential with the shape of a two-level system (TLS) in its symmetric ground-state configuration.

$Q(\tau)$  is the one-dimensional *space-time* hopping path followed by the atom which moves between two equilibrium positions located at  $\pm Q_0$ .  $\tau_0$  is the bare hopping time for hopping between the two minima of the TLS and  $t_i$  is the instant at which the  $i$ th hop takes place. An atomic path is characterized by the number  $2n$  of hops, by the set of  $t_i$  ( $0 < i \leq 2n$ ) and by  $\tau_0$ . In the last of equations (1), we assume that the class of  $\tau$ -linear paths yields the main contribution to the full partition function of the interacting system. The closure condition on the path is given by  $(2n - 1)\tau_s + 2n\tau_0 = \beta$ , where  $\beta$  is the inverse temperature and  $\tau_s$  is the time for which one atom remains in a well. The interaction is described by  $H_{int}(\tau)$  with  $\lambda$  being the strength of coupling between the TLS and the polaron;  $\lambda Q(\tau)$  is the renormalized (versus time) tunnelling energy which allows one to introduce the  $\tau$ -dependence in the interacting Hamiltonian [15].

Following a method previously developed [16] in the study of the Kondo problem, we multiply  $\lambda Q(\tau)$  by a fictitious coupling constant  $s$  ( $0 \leq s \leq 1$ ) and, by differentiating with respect to  $s$ , one derives the single-path contribution to the partition function of the system:

$$\ln\left(\frac{Z(n, t_i)}{Z_0}\right) = -2\lambda \int_0^1 ds \int_0^\beta d\tau Q(\tau) \lim_{\tau' \rightarrow \tau^+} G(\tau, \tau')_s, \tag{2}$$

where  $Z_0$  is the partition function related to  $H_0$  and  $G(\tau, \tau')_s$  is the full propagator for polarons satisfying Dyson's equation:

$$G(\tau, \tau')_s = G^0(\tau, \tau') + s \int_0^\beta dy G^0(\tau, y)\lambda Q(y)G(y, \tau'). \tag{3}$$

The polaronic free propagator  $G^0$  can be derived exactly in the model described by equations (1) [17]. We get the full partition function of the system by integrating over the

times  $t_i$  and summing over all possible even numbers of hops:

$$Z_T = Z_0 \sum_{n=0}^{\infty} \int_0^{\beta} \frac{dt_{2n}}{\tau_0} \int_0^{t_2-\tau_0} \frac{dt_1}{\tau_0} \exp[-\beta E(n, t_i, \tau_0)] \quad (4)$$

$$\beta E(n, t_i, \tau_0) = \Lambda - (K^A + K^R) \sum_{i>j}^{2n} \left( \frac{t_i - t_j}{\tau_0} \right)^2$$

with  $E(n, t_i, \tau_0)$  being the single-path atomic energy.  $\Lambda$ , which is a function of the input parameters, is not essential here, while the second addendum in equation (4) is *not local in time* as a result of the retarded polaronic interactions between successive atomic hops in the double-well potential.  $K^A$  and  $K^R$  are the single-path coupling strengths containing the physics of the interacting system.  $K^A$  (negative) describes the polaron–polaron attraction mediated by the local instability and  $K^R$  (positive) is related to the repulsive scattering of the polaron by the TLS. Computation of  $E(n, t_i, \tau_0)$  and its derivative with respect to  $\tau_0$  shows that the largest contribution to the partition function is given by the atomic path with  $\tau_s = 0$ . The atom moving back and forth in the double well minimizes its energy if it takes the path with the highest  $\tau_0$ -value allowed by the boundary condition—that is, with  $(\tau_0)_{max} = (2nK_B T)^{-1}$ . This result, which is general, provides a criterion for determining the set of dominant paths for the atom at any temperature. Then, the effective interaction strengths  $\langle K^A \rangle$  and  $\langle K^R \rangle$  can be obtained as functions of  $T$  by summing over  $n$  the dominant path contributions:

$$\langle K^A \rangle = -(\lambda Q_0)^2 B^2 \exp\left(2 \sum_q A_q\right) \sum_q A_q \omega_q^2 \tilde{f} \quad (5)$$

$$\langle K^R \rangle = -\beta (\lambda Q_0)^3 B^3 \exp\left(3 \sum_q A_q\right) \sum_q A_q \omega_q^2 \tilde{f}$$

with

$$B = (n_F(\bar{\epsilon}) - 1) \exp\left(-g \sum_q \coth(\beta \omega_q / 2)\right) \quad A_q = 2g \sqrt{N_q(N_q + 1)}.$$

$N_q$  is the phonon occupation factor and  $n_F(\bar{\epsilon}(g))$  is the Fermi distribution for polarons.

$$\tilde{f} = \sum_{n=1}^N (\tau_0)_{max}^4$$

and  $N$  is the cut-off on the number of hops in a path. The particular form of  $(\tau_0)_{max}$  suggests that many-hop paths are the excitations of relevance at low temperatures whereas paths with a low number of hops provide the largest contribution to the partition function at high temperatures. Since the effective couplings which determine the resistivity depend on  $(\tau_0)_{max}^4$ , and hence on  $N^{-3}$  (through  $\tilde{f}$ ), a relatively small cut-off ( $N \simeq 4$ ) ensures numerical convergence of equations (5) over the whole temperature range. On the other hand, the non-retarded term  $\Lambda$  in equation (4) has a slower  $1/N$  behaviour; therefore a larger cut-off should be taken at low temperatures where the computation of equilibrium properties such as the specific heat is strongly influenced by many-hop atomic paths between the minima of the double-well excitations.

The lattice Hamiltonian is that of diatomic sites whose intramolecular vibrations can favour trapping of the charge carriers [18]. The *intramolecular* frequency  $\omega_0$  largely determines the size of the lattice distortion associated with polaron formation [19] while the dispersive features of the phonon spectrum controlled by the first-neighbour ( $\omega_1$ ) and second-neighbour ( $\omega_2$ ) *intermolecular* couplings are essential for computing the polaron properties both in the ground

state and at finite temperatures [20]. The range of the intermolecular forces is extended to the second-neighbour shell, since these couplings remove the phonon mode degeneracy (with respect to dimensionality) at the corners of the Brillouin zone, thus permitting one to estimate with accuracy the relevant contributions of high-symmetry points to the momentum-space summations [21]. Then the characteristic frequency  $\bar{\omega}$ , which we choose as the zone-centre frequency, is

$$\bar{\omega}^2 = \omega_0^2 + z\omega_1^2 + z_{nnn}\omega_2^2$$

where  $z$  is the coordination number and  $z_{nnn}$  is the next-nearest-neighbour number. Hereafter we take frequency values which are appropriate to systems with rather sizable phonon spectra.

We turn now to computing the electrical resistivity due to the polaronic charge-carrier scattering by the impurity potential with an internal degree of freedom provided by the TLS. Assuming s-wave scattering, one gets [22, 23]

$$\begin{aligned} \rho &= \rho_0 \sin^2 \eta \\ \rho_0 &= \frac{3n_s}{\pi e^2 v_F^2 (N_0/V)^2 \hbar} \end{aligned} \quad (6)$$

where  $n_s$  is the density of TLSs which act as scatterers,  $v_F$  is the Fermi velocity,  $V$  is the cell volume,  $N_0$  is the electron density of states,  $e$  is the charge and  $\hbar$  is the Planck constant. The phase shift  $\eta$  of the electronic wave function at the Fermi surface is related to the effective interaction strengths  $\langle K^A \rangle$  and  $\langle K^R \rangle$ .

The input parameters of the model number six—that is, the three molecular force constants,  $g$ ,  $D$  and the bare energy  $\lambda Q_0$ .  $Q_0$  can be chosen as  $\simeq 0.05 \text{ \AA}$  consistently with reported values in the literature on TLSs which are known to exist in glassy systems [24–27], amorphous metals [28], A15 compounds and probably in some cuprate superconductors [29–31]. In these systems the origin of the TLSs is not magnetic. The bare electronic band  $D$  is fixed at 0.1 eV.

Let us start by studying (figure 1) the resistivity behaviour in a 3D lattice as a function of the overall electron–phonon coupling  $g$ .  $\lambda$  is fixed at  $700 \text{ meV \AA}^{-1}$ , which means a bare tunnelling energy of  $\simeq 35 \text{ meV}$ , and the molecular force constants are  $\omega_0 = 60 \text{ meV}$ ,  $\omega_1 = 50 \text{ meV}$  and  $\omega_2 = 20 \text{ meV}$ , respectively. At low temperatures  $\rho(T)$  approaches the unitary limit for any of the four  $g$ -values, thus displaying the peculiar effect of the anharmonic potential with an internal degree of freedom. At  $T \simeq 150 \text{ K}$ ,  $\rho$  develops a  $g$ -dependent broad peak which softens and finally disappears with increasing  $g$  in the strong-coupling regime. We note that at  $g > 1$  the polaron energy becomes smaller than the atomic tunnelling energy; hence polaron

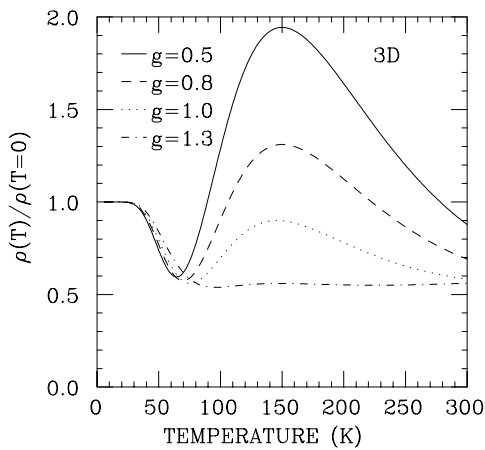


**Figure 1.** Electrical resistivity normalized to the residual ( $T = 0$ ) resistivity for four values of electron–phonon coupling  $g$ . The bare TLS energy  $\lambda Q_0$  is 35 meV. The force constants which control the phonon spectrum in the 3D lattice are:  $\omega_0 = 60 \text{ meV}$ ,  $\omega_1 = 50 \text{ meV}$ ,  $\omega_2 = 20 \text{ meV}$ .

scattering by the TLS is essentially diagonal. In contrast, in the intermediate-coupling regime ( $g$  in the range 0.5–1), the incoming polaron can release a sufficiently large amount of energy, off-diagonal scattering by the impurity potential prevails and a broad resonance peak emerges. At weaker  $g$  the polaronic picture would lose any validity.

Next we turn to considering the effect of the lattice dynamics on the  $\rho$  versus  $T$  behaviour. In figures 2 and 3, the normalized resistivities are reported for the 1D and 2D molecular lattices, respectively. Let us set  $g = 1$ , which ensures both polaron formation and the presence of the resonance peak in 1D and 2D systems while the tunnelling energy (as in figure 1) is in the range of the values estimated by EXAFS investigations on high- $T_c$  systems with double site distributions for the apical oxygen atoms [29, 32]. By taking  $\omega_0 = 60$  meV and  $\omega_1 = 50$  meV we choose for the first-neighbour intermolecular coupling model a characteristic phonon energy  $\bar{\omega} \simeq 0.1$  eV. This choice allows us: (i) to treat correctly the ground-state polaron properties versus dimensionality [21], (ii) to reproduce the sizable phonon energy of the  $c$ -axis polarized mode due to apex oxygen vibrations coupled to the holes in the Cu–O planes of  $\text{YBa}_2\text{Cu}_3\text{O}_{7-\delta}$ . In underdoped compounds (whose  $c$ -axis resistivity displays the unusual non-metallic behaviour), this mode appears enhanced in energy [33]. Although our simple cubic lattice does not account for the details of the structural effects of YBCO, we are in the appropriate range of parameters for capturing the main features of the lattice polarons

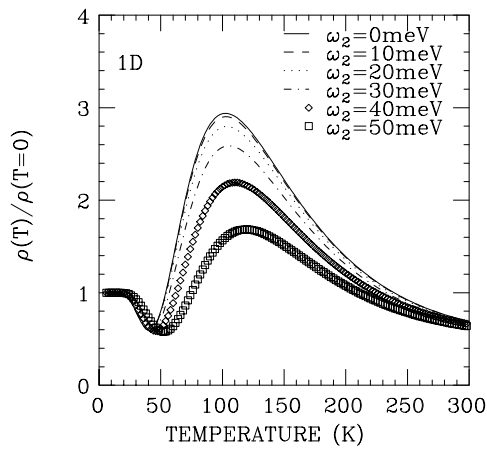


**Figure 2.** The 1D electrical resistivity as a function of the second-neighbour intermolecular force constant.  $g = 1$ .  $\lambda Q_0$ ,  $\omega_0$  and  $\omega_1$  are as in figure 1.

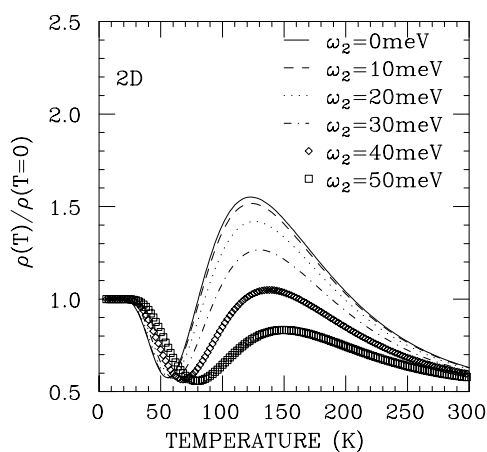


**Figure 3.** The 2D electrical resistivity as a function of the second-neighbour intermolecular force constant.  $g = 1$ .  $\lambda Q_0$ ,  $\omega_0$  and  $\omega_1$  are as in figure 1.

scattered by local instabilities in those compounds. The role of the second-neighbour couplings is emphasized in figures 2 and 3 by varying  $\omega_2$ , which however should not exceed  $\omega_1$ . On increasing  $\omega_2$ , the polaron spreads in real space and becomes lighter. Accordingly the height of the peak decreases. We also note that the strength of the intermolecular forces influences the position of the peak versus temperature which results from a balance between competing attractive and repulsive interactions (equations (5)). For fixed parameters, the height of the 1D peak is roughly twice that of the 2D one. Comparing the dotted 2D curve ( $\omega_2 = 20$  meV) with the corresponding case ( $g = 1$  plot) in figure 1, one sees that the 3D peak is further reduced and its absolute value lies below the residual resistivity value.

The dynamics of the TLS and its coupling to the charge carrier strongly affect the transport in any dimensionality, as figure 4 makes evident. When  $\lambda$  is small (i.e. below  $300 \text{ meV \AA}^{-1}$  in 1D), the polaron and TLS are weakly coupled, off-diagonal scattering is unlikely to occur and the conductivity is metallic-like. On increasing  $\lambda$ , the atomic tunnelling energy becomes

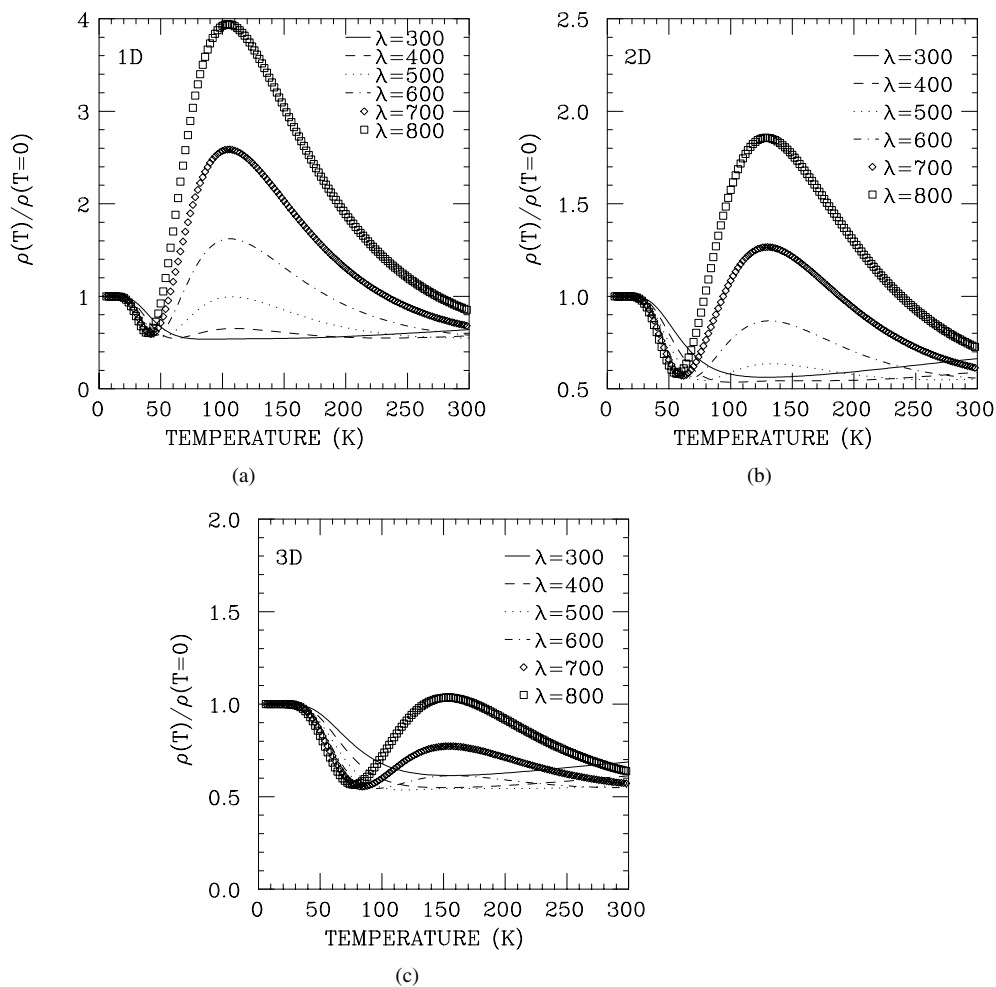


**Figure 4.** Electrical resistivities for six values of the polaron–TLS coupling  $\lambda$  in units  $\text{meV \AA}^{-1}$ .  $g = 1$ .  $\omega_0 = 60$  meV,  $\omega_1 = 50$  meV,  $\omega_2 = 30$  meV. (a) One dimension; (b) two dimensions; (c) three dimensions.

of the order of the polaron energy and the conditions for resonant scattering are established. Note that on varying  $\lambda$  the resistivity peak does not shift versus temperature while the threshold value of  $\lambda$  for the appearance of metallic conductivity is larger in higher dimensionality. This means that 3D systems can sustain a larger degree of anharmonicity (than low-dimensional systems) and still exhibit metallic transport properties, while trapping of the charge carrier by the anharmonic impurity potential is favoured in 1D. It is this trapping which causes the broad resistivity peak and non-metallic transport at  $T$  larger than  $\simeq 100$  K in 1D.

We investigate further the effect of the molecular forces (figure 5) by *increasing* the *intra*-molecular energy and *decreasing* the *inter*molecular energies with respect to those of figure 4. The 1D peak (compare figure 5(a) and figure 4(a)) is reduced for any  $\lambda$ -value, whereas the 2D and 3D peaks are here larger than in figures 4(b) and 4(c) respectively. The reason is the following: in 1D, the intramolecular coupling is dominant because of the low coordination number; as a result, on enhancing  $\omega_0$  the carriers become lighter and the absolute resistivity

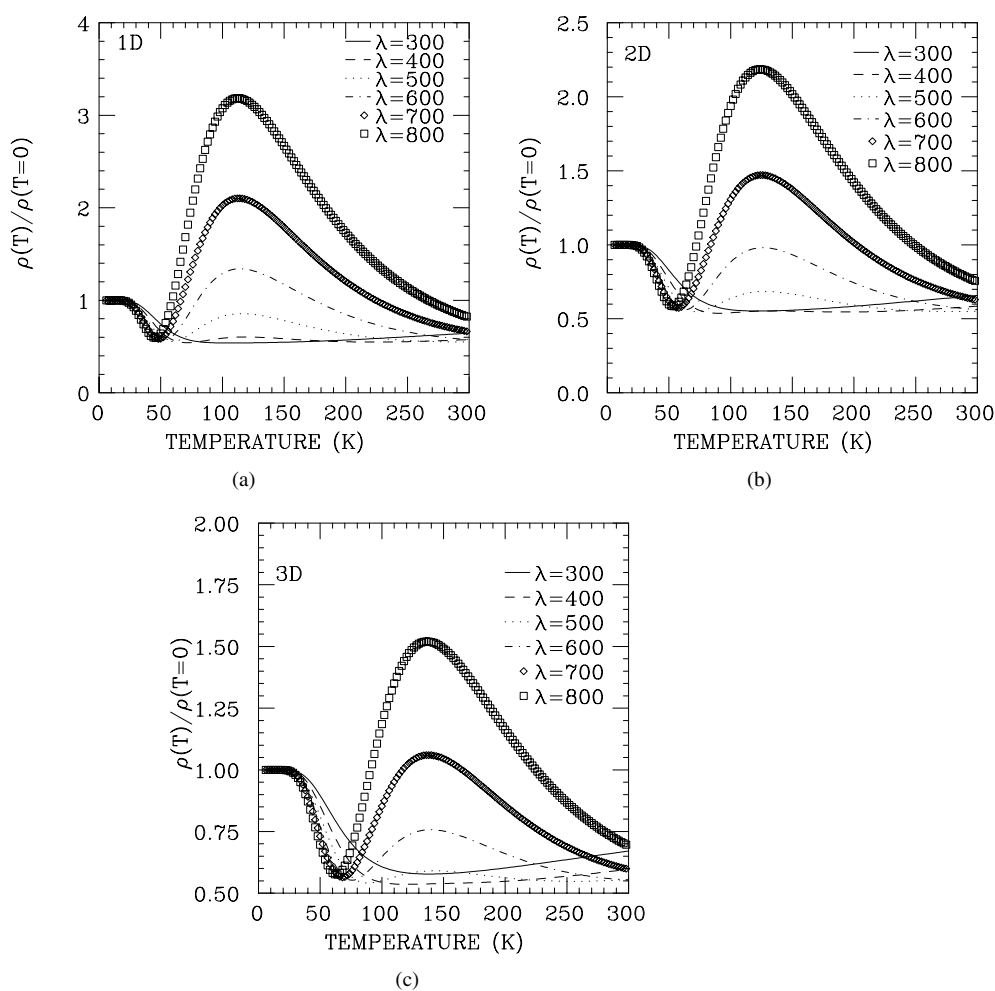


**Figure 5.** Electrical resistivities for six values of the polaron–TLS coupling  $\lambda$  in units  $\text{meV \AA}^{-1}$ .  $g = 1$ .  $\omega_0 = 80$  meV,  $\omega_1 = 40$  meV,  $\omega_2 = 20$  meV. (a) One dimension; (b) two dimensions; (c) three dimensions.



is reduced. In contrast, in 2D and mostly in 3D, long-range effects are more effective; hence, the stronger  $\omega_0$  (with respect to the values for figure 4) is more than balanced by the weaker  $\omega_1$  and  $\omega_2$ ; as a result, the characteristic 2D and 3D phonon frequencies are smaller, polarons become less mobile and the resistivity peaks are accordingly higher.

### 3. Conclusions

The path integral formalism has been applied to study the time-retarded interaction problem for a polaron scattered by a local anharmonic potential in a lattice of diatomic molecules. I have derived the full partition function of the system and obtained analytically the effective coupling strengths as a function of temperature. The electrical resistivity has been computed for any lattice dimensionality for a large choice of input parameters. The strength of the overall electron–phonon coupling ( $g$ ), the strength of the polaron–local potential coupling ( $\lambda$ ) and the strength of the molecular forces interfere, giving rise to a rich variety of resistivity behaviours versus temperature. As a main feature, when the conditions for resonant scattering between the polaron and local double-well potential are fulfilled, a broad resistivity peak shows up in the 100–150 K range. However, the shape of the peak essentially depends on the dynamics of the local potential (tuned by  $\lambda$ ) and, for sufficiently low atomic tunnelling energies, metallic conductivity conditions are recovered. Generally, in 3D the resistivity maximum is less pronounced than in low dimensionality and, for sufficiently strong intermolecular couplings, the height of the peak lies below the residual resistivity value, therefore being hardly visible in experiments. On the other hand, in 1D and 2D, the maximum can easily become larger than the residual resistivity by a factor of  $\simeq 3$ –4 for realistic choices of tunnelling energies and lattice force constants. Then, non-metallic resistivities can be expected in low-dimensional polaronic systems with local lattice instabilities at least for temperatures above  $\simeq 100$  K. As a final remark, one should add that, while the *intramolecular* and *intermolecular* energies have been varied throughout the paper as apparently independent parameters, their values for real systems can be obtained (for instance) by a least-squares procedure of fitting to experimentally known physical quantities [34].

### Acknowledgments

I am grateful to V R Sobol and O N Mazurenko for helpful collaboration. A NATO-CNR grant is acknowledged.

### References

- [1] Emin D and Holstein T 1976 *Phys. Rev. Lett.* **36** 323
- [2] De Raedt H and Lagendijk A 1983 *Phys. Rev. B* **27** 6097  
De Raedt H and Lagendijk A 1984 *Phys. Rev. B* **30** 1671
- [3] Kabanov V V and Mashtakov O J 1993 *Phys. Rev. B* **47** 6060
- [4] Kopidakis G, Soukoulis C M and Economou E N 1995 *Phys. Rev. B* **51** 15 038
- [5] de Mello E and Ranninger J 1997 *Phys. Rev. B* **55** 14 872
- [6] Kalosakas G, Aubry S and Tsironis G P 1998 *Phys. Rev. B* **58** 3094
- [7] Kostur V N and Allen P B 1997 *Phys. Rev. B* **56** 3105
- [8] Alexandrov A S and Mott N F 1994 *Rep. Prog. Phys.* **57** 1197
- [9] Yarlagadda S 2000 *Preprint cond-mat/0010198*
- [10] Devreese J T 1996 *Encyclopedia of Applied Physics* vol 14 (New York: Wiley–VCH) pp 383–409
- [11] Romero A H, Brown D W and Lindenberg K 1999 *Phys. Rev. B* **60** 14 080
- [12] Voulgarakis N K and Tsironis G P 2001 *Phys. Rev. B* **63** 14 302

- [13] Mihailović D, Ruani G, Kaldis E and Müller K A (ed) 1995 *Anharmonic Properties of High  $T_c$  Cuprates* (Singapore: World Scientific)
- [14] Palles D, Poulakis N, Liarakapis E, Conder K, Kaldis E and Müller K A 1996 *Phys. Rev. B* **54** 6721
- [15] Zoli M 1991 *Phys. Rev. B* **44** 7163
- [16] Hamann D R 1970 *Phys. Rev. B* **2** 1373
- [17] Zoli M 1999 *Proc. 6th Int. Conf. on Path Integrals from peV to TeV—50 Years after Feynman's paper* (Singapore: World Scientific) p 478
- [18] Holstein T 1959 *Ann. Phys., NY* **8** 325
- [19] Alexandrov A S and Kornilovitch P E 1999 *Phys. Rev. Lett.* **82** 807
- [20] Zoli M 2000 *J. Phys.: Condens. Matter* **12** 2783
- [21] Zoli M 2000 *Phys. Rev. B* **61** 14 523
- [22] Mahan G D 1981 *Many Particle Physics* (New York: Plenum)
- [23] Yu C C and Anderson P W 1984 *Phys. Rev. B* **29** 6165
- [24] Anderson P W, Halperin B I and Varma C H 1971 *Phil. Mag.* **25** 1
- [25] Philipps W A 1972 *J. Low Temp. Phys.* **7** 351
- [26] Fessatidis V, Mancini J D, Massano W J and Bowen S P 2000 *Phys. Rev. B* **61** 3184
- [27] Zawadowski A, von Delft J and Ralph D C 1999 *Phys. Rev. Lett.* **83** 2632
- [28] Cochrane R V, Harris R, Strom-Olsen J and Zuckerman M J 1975 *Phys. Rev. Lett.* **35** 676
- [29] Mustre de Leon J, Conradson S D, Batistic I and Bishop A R 1991 *Phys. Rev. B* **44** 2422
- [30] Saiko A P and Gusakov V E 1999 *JETP* **89** 92
- [31] Menuschenkov A P and Klementev K V 2000 *J. Phys.: Condens. Matter* **12** 3767
- [32] Haskel D, Stern E A, Hinks D G, Mitchell A W and Jorgensen J D 1997 *Phys. Rev. B* **56** R521
- [33] Timusk T, Homes C C and Reichardt W 1995 *Anharmonic Properties of High  $T_c$  Cuprates* ed D Mihailović, G Ruani, E Kaldis and K A Müller (Singapore: World Scientific) p 171
- [34] Zoli M 1991 *J. Phys.: Condens. Matter* **3** 6249